# Multiphoton ionization as time-dependent tunneling

Klaus Ergenzinger*
*Institut für Theoretische Physik, Universität Zürich, Winterthurerstrasse 190, CH-8057 Zürich, Switzerland*
(Received 17 April 1996)

A semiclassical approach to ionization by an oscillating field is presented. An asymptotic analysis is performed with respect to a quantity $h$, defined (up to a factor) as the ratio of photon energy to ponderomotive energy. This $h$ appears formally equivalent to Planck's constant in a suitably transformed Schrödinger equation and allows us to formally use semiclassical methods. Systematically, a picture of tunneling wave packets in complex time is developed, which by interference account for the typical ponderomotive features of ionization curves. For a one-dimensional $\delta$-function atom, these analytical results are compared to numerical simulations [Scharf, Sonnenmoser, and Wreszinski, Phys. Rev. A **44**, 3250 (1991)] and are shown to be in good agreement. [S1050-2947(97)01201-8]

PACS number(s): 32.80.Rm, 03.65.Sq

## I. INTRODUCTION

A lot of effort was dedicated recently to a better understanding of ionization by strong laser fields (reviews, e.g., in [2,3]), especially since the discovery of nonperturbative phenomena, like above-threshold ionization (ATI) (for a review see [4]), the sensitivity of ionization rates, and stabilization in superintense fields [5–7].

But there succeeded no analytical solution for the simplest model, i.e., a one-dimensional electron bound by an attractive $\delta$ potential in the presence of an oscillating electric field. One of the main reasons is that there exist two separate regions. The binding potential dominates inside the atomic core, whereas the electric field dominates outside the core (this is also the main point that makes perturbation theory work so poorly). For both regions, the distinct propagators are exactly known, but they cannot be combined to solve the ionization problem exactly.

This problem can be treated nonperturbatively by a semiclassical approach, which we will use to construct the semiclassical propagator explicitly for such a one-dimensional $\delta$-function atom. The choice of this model has three advantages: first, there is a clear distinction between inside and outside the atom. So there does not exist any intermediate region. Second, there is only one bound state for the $\delta$ potential (as in $H^-$), so there arise no difficulties with intermediate resonances and induced resonances by ac-Stark shift, as it happens in real atoms. Third, the exact problem can be reduced to a Volterra type integral equation in time, for which accurate numerical solutions can be computed [1] and which allows precise tests.

The one-dimensional $\delta$-function model has shown to be useful for real physical systems, e.g., $H^-$ in a static electric field [8]. For high electric fields, in which we are interested, the driven motion of the electron along the field direction is much more important than the other degrees of freedom, so that the essential dynamics reduces to one dimension.

The above described problem (as well as its more general settings in three dimensions with more realistic binding potentials) has been treated in the literature in several ways. The so-called Keldysh-Faisal-Reiss (KFR) approach [9–11] consists in expressing the exact propagator $\hat{U}$ in terms of the known Volkov propagator $\hat{U}^V$ [12] (for a free electron in the electromagnetic field) and in terms of $V_\delta$, the atomic binding potential: $\hat{U}=\hat{U}^V-i\hat{U}^V V_\delta \hat{U}$. The unknown $\hat{U}$ on the right-hand side is approximated by $\hat{U}^V$ (equivalent to the Born approximation), and matrix elements for ionization are calculated between the ground state and so-called Volkov states [12] in the continuum. This approach has been refined and extended by many authors, and we will compare our results with two such typical extensions [13,14].

Another approach, the so-called two-step model [15–17], clearly distinguishes between ionization first and classical propagation in the (laser) field afterwards. This proved to be very useful especially in calculating high-harmonic generation [18]. This separation into two steps will be used in the following, but now justified in a fully semiclassical context.

In addition, there exist several other approaches. A very common method is using the Floquet theory [19–21], which explicitly incorporates the periodicity of the time-dependent Hamiltonian. Our issue here is not to obtain better results for a simple model, but to gain better physical insight into the mechanisms of ionization processes using semiclassical methods.

This paper is organized as follows: After basic definitions (Sec. II), we show characteristic elements of generic ionization curves (Sec. III), which we want to understand semiclassically. Using a ''sum over classical paths'' technique, the total semiclassical propagator is constructed by identifying the paths which are relevant for ionization. First we construct the propagator for the part remaining bound (Sec. IV), and second we construct the propagator for the free wave packets stemming from time-dependent tunneling in complex time (Sec. V). Using the total semiclassical propagator (Sec. VI), the total ionization rate is derived and compared to numerical simulations as well as to other theories in the literature (Sec. VII). Finally, in Appendix A, it is shown how these results can be generalized to other binding potentials.

*Electronic address: erg@physik.unizh.ch

 

## II. BASICS

### A. Definition of the model

We want to study the ionization of a one-dimensional $\delta$-function atom with binding potential $V_\delta = -\alpha\delta(x)$, which possesses exactly one bound state with binding energy $E_0 = -\alpha^2/2$ (for the three-dimensional analog cf. [22] and the solutions by [23,24], using complex quasienergies). This atom is exposed to an oscillating electric field $V_0 = -\mu x\cos(\omega t)$ in the so-called dipole approximation. The parameter $\alpha$ represents the strength of the binding potential, $\mu$ is the amplitude of the applied electric field, and $\omega$ is its angular frequency. The Schrödinger equation in atomic units ($\hbar = m = 1$) is

$$i\frac{\partial}{\partial t}\psi = \left[ -\frac{1}{2}\frac{\partial^2}{\partial x^2} - \alpha\delta(x) - \mu x\cos(\omega t)\right]\psi. \tag{1}$$

From these three parameters, there can be derived (due to the scaling properties of the one-dimensional $\delta$ potential) two independent, meaningful, and dimensionless quantities: first, $z = \mu^2/(4\omega^3)$, which is the ratio of ponderomotive energy $U_{pond} = \mu^2/(4\omega^2)$ to photon energy $\omega$ . $U_{pond}$ is the mean kinetic energy of a free electron in an oscillating field. And, second, the so-called Keldysh factor [9] $\gamma = \alpha\omega/\mu$, which is the ratio of the (adiabatic) tunneling time to the period of the applied field. This $\gamma$ characterizes the ionization process; $\gamma \ll 1$ corresponds to (adiabatic) tunneling, and $\gamma \gg 1$ is better described in a pure multiphoton frame [25,26].

These are the two quantities by which the model will be described below. A third, but no more independent quantity is $n_{io}$, the ratio of binding energy $E_0$ to photon energy

$$n_{io} = \alpha^2/(2\omega) = 2\gamma^2 z. \tag{2}$$

### B. Transformation of the Schrödinger equation

With the following coordinate and time transformation, we cast the above Schrödinger equation (1) in a very suitable form:

$$x' = \frac{\omega^2}{\mu}x, \quad t' = \omega t. \tag{3}$$

Using the scaling relation $\delta(ax) = \delta(x)/|a|$ (which is identical to the scaling behavior of the Coulomb potential) and omitting the primes, we obtain

$$ih\frac{\partial}{\partial t}\psi = \left( -\frac{1}{2}h^2\frac{\partial^2}{\partial x^2} - h\gamma\delta(x) - x\cos(t)\right)\psi. \tag{4}$$

Here $h := \omega^3/\mu^2 = 1/(4z)$ is written very suggestively to indicate that we have obtained a parameter $h$ formally equivalent to Planck's constant $\hbar$ in ordinary quantum mechanics [using Système International (SI) units]. Of course we can give $h$ any value we like. Restricting ourselves to strong fields with $U_{pond} \gg \omega$, i.e., $z \gg 1$, $h$ can get arbitrarily small. This will allow us to use the normal semiclassical methods, exploiting the formal analogy between the parameter $h$, introduced above, and Planck's constant $\hbar$. Quite remarkable is the appearance of the factor $h$ in front of the binding $\delta$ potential, its implications in the semiclassical limit will be derived below. For the three-dimensional $\delta$ potential $\delta^3(\mathbf{r})$ or the regularized potential $\delta^3(\mathbf{r})\,(\partial/\partial\mathbf{r})\,\mathbf{r}$, such a transformation is no longer possible because of the different scaling behavior.

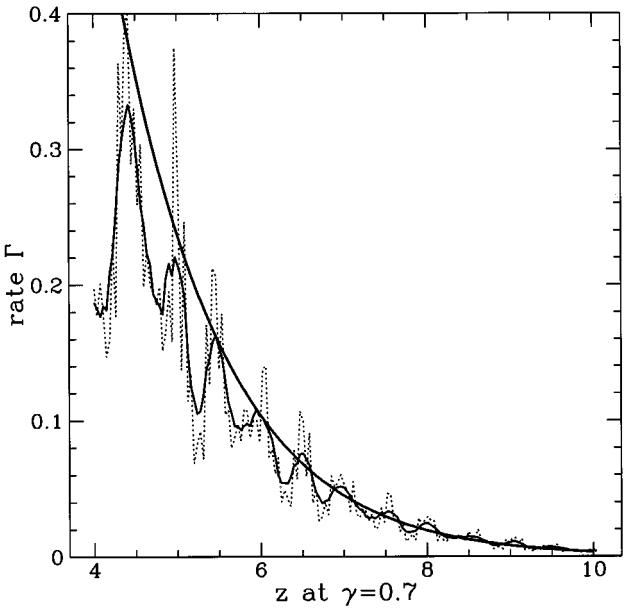


FIG. 1. Numerical ionization rates, raw (dotted) and smoothed (thicker) vs number of ponderomotive photons $z$, compared with WKB background (thick, smooth decaying curve). The Keldysh parameter $\gamma$ and not the depth of the binding potential is kept fixed.

The (normalized) ground-state wave function for the one-dimensional $\delta$-function atom without an applied external field is

$$\psi_0(x) = \left(\frac{\gamma}{h}\right)^{1/2}\exp\left( -\frac{\gamma}{h}\left|x\right|\right), \tag{5}$$

$$\hat{H}_0\psi_0 = -\frac{\gamma^2}{2}\psi_0, \tag{6}$$

$$\psi_0(x,t) = \psi_0(x)\exp\left( i\frac{\gamma^2}{2h}t\right).$$

For small $h$, this leads to a strong localization of the wave function $\psi_0$ around the origin. In the limiting case $h \to 0$, $\psi_0(x)$ approaches (appropriately scaled) the spatial Dirac $\delta$ function

$$\frac{1}{2}\left(\frac{\gamma}{h}\right)^{1/2}\psi_0(x) \to \delta(x). \tag{7}$$

In the following, this approximation will be used only for the calculation of scalar products, so that no mathematical ambiguities will arise.

## III. PROMINENT SEMICLASSICAL FEATURES IN IONIZATION RATES

The ionization rates from a numerical analysis [1] of this model show certain characteristic features. In Fig. 1, we can see the raw results (dotted), these results smoothed (thicker),

and the adiabatically averaged WKB value [thick and monotonically decreasing, see Eq. (16)]. The ionization rate $\Gamma$ is shown against $z$, the ratio of ponderomotive energy over photon energy. The WKB rate accounts fine for the background, but on the actual rate, there is a modulation and a lot of fine structure superposed. The (slow) modulation becomes obvious after having smoothed the raw data (using a Savitzky-Golay filter technique).

The cycle length of this modulation can be understood by the so-called channel closing arguments [27], but there is up to now no argument for the amplitude of this modulation. The $k$th channel means a multiphoton ionization by $k$ photons with energy balance (here in atomic units)

$$k\omega = n_{io}\omega + z\omega + E_{kin}, \tag{8}$$

$n_{io}\omega$ is the binding energy, $z\omega$ is the ponderomotive energy $U_{pond}$, and $E_{kin}$ is the additional kinetic energy the electron gains in this ionization process. This channel is energetically only allowed for $E_{kin} \geqslant 0$, otherwise it is forbidden.

The threshold $z_k$ for the $k$th channel is defined using the condition $E_{kin}=0$. In terms of $\gamma$ and $z_k$, Eq. (8) at threshold is

$$k = 2\gamma^2 z_k + z_k \tag{9}$$

and the specific value $z_k$ at threshold becomes

$$z_k = \frac{k}{1+2\gamma^2}, \tag{10}$$

yielding cycles with length $\Delta z = 1/(1+2\gamma^2)$. In Fig. 1, this yields a cycle of approximately 0.5 for $\gamma = 0.7$.

An important point to note is that the numerical results give strong evidence for regular behavior of ionization rates $\Gamma$ at threshold, whereas the usual prediction of appropriate theories (e.g., those of the KFR type) is a divergence at threshold.

The features described above are definitely not restricted to the $\delta$-function atom alone. Numerical simulations for various model potentials in the literature exhibit similar features, often with remarkable quantitative correspondence (see Fig. 8 in [1], comparing the $\delta$-function atom to an atom with a smoothed binding potential $V(x) = -\exp(-|x|)/\sqrt{x^2+x_0^2}$ as used by Greenwood and Eberly [28]).

In the following, a semiclassical theory is derived that accounts for the information contained in smoothed rates. The WKB background and the properties of the modulation are contained in a single, divergence free theory, which constructs the propagator using the semiclassical sum over paths, cf., e.g., [29].

## IV. QUASIENERGIES

### A. Calculation of WKB coefficient

The main effect of applying an external field to an atom is that the bound state becomes metastable and tunneling can occur. In the static case, this tunneling rate $D$ can be approximated using the usual WKB coefficient for the corresponding barrier. For a linear potential barrier $V(x) = -\eta x$ and a given (negative) energy $E_0$, the well-known expression for $D$ is

$$D(\eta) \approx \exp\left( -\frac{2}{h}\int_0^{-E_0/\eta} |p(x)|\,dx \right). \tag{11}$$

Using the (imaginary) local momentum $p(x) = \sqrt{2(E_0+\eta x)}$ and the ground-state energy $E_0 = -\gamma^2/2$, this evaluates to

$$D(\eta) \approx \exp\left( -\frac{2}{3}\frac{\gamma^3}{\eta h} \right). \tag{12}$$

Of course, this approach gives only the exponential part. But since the preexponential part is well known from the literature for this simple case (e.g., [14,30]), we can take it from there. This factor is just twice the atomic frequency, in our units $2E_0/h$

$$D(\eta) = \frac{\gamma^2}{h}\exp\left( -\frac{2}{3}\frac{\gamma^3}{\eta h} \right). \tag{13}$$

If we consider a time-dependent external field, the parameter $\eta$ becomes time dependent too and represents the instantaneous strength of the electric field: $\eta = |\cos(t)|$. If the tunneling process occurs on a much shorter time scale than the period $2\pi$ of the oscillation, it is a good idea to consider the ionization taking place adiabatically. So we calculate the instantaneous ionization rate $D(|\cos(t)|)$ and average it over a whole period. This case corresponds to $\gamma \ll 1$, i.e., the Keldysh factor must be quite small.

In calculating the cycle average $\overline{D}$ over a period of the external field, one has to integrate and to normalize subsequently

$$\overline{D} = \frac{1}{2\pi}\int_0^{2\pi} \frac{\gamma^2}{h}\exp\left( -\frac{2}{3}\frac{\gamma^3}{|\cos(t)|h} \right) dt. \tag{14}$$

Because we want to examine the asymptotic case $h \to 0$, we best evaluate this integral using the method of steepest descent (also called the saddle-point integration). The derivation of the exponential argument with respect to time $t$ yields

$$\frac{d}{dt}\left( -\frac{2}{3}\frac{\gamma^3}{\cos(t)} \right) = -\frac{2}{3}\gamma^3\frac{\sin(t)}{\cos(t)^2}. \tag{15}$$

The relevant times are the zeros of this expression, i.e., all multiples of $\pi$. These are the instants where the electric-field strength $|\cos(t)|$ is at a maximum. For symmetry reasons, all these instants are equivalent and it is sufficient to evaluate the above integral at one such instant using the method of steepest descent. The result is

$$\overline{D} = \left( \frac{3h}{\pi\gamma^3} \right)^{1/2} \frac{\gamma^2}{h}\exp\left( -\frac{2}{3}\frac{\gamma^3}{h} \right) \tag{16}$$

$$= \left( \frac{3h}{\pi\gamma^3} \right)^{1/2} D(\eta = 1). \tag{17}$$

This shows that the average $\overline{D}$ is the instantaneous ionization rate at maximum field strength, up to a preexponential factor.

Note that the method of steepest descent becomes exact in the limit of vanishing $h$. This allows a very interesting interpretation. In this case, the ionization effectively takes place

only in the vicinity of the instants with maximal field strength ($\eta=1$). This means that there exist ionization bursts, separated by half a period, between which practically no other ionization occurs. In the following, this property will be used to construct a scenario of propagating wave packets. These wave packets emerge at times $t=k\pi$, propagate freely afterwards, and interfere with one another and with the part of the wave function remaining bound.

### B. ac-Stark effect

The second effect of applying an external field is the so-called Stark effect, in the time-dependent case called the ac-Stark effect. We will treat this effect adiabatically too (cf. [31]); the well-known value (e.g., [14,30,32]) for the instantaneous energy shift $E^{\mathrm{ac}}$ is $E^{\mathrm{ac}}(\eta)=-5h^2\eta^2/(8\gamma^4)$. Cycle averaging results in

$$\overline{E^{\mathrm{ac}}}=\frac{1}{2}E^{\mathrm{ac}}(\eta=1)=-\frac{5h^2}{16\gamma^4}. \tag{18}$$

This effect means an additional phase factor in the propagator $\exp(-i\hat{H}t/h)$, whereas the tunneling rate, calculated by taking absolute squares of the wave function, is not affected by $E^{\mathrm{ac}}$. Note that the influence of Eq. (18) will be quite small in the following because of its proportionality to $h^2$.

In order to express tunneling and Stark shift together, it is useful to write the exponential decay of the bound state using an imaginary contribution $E^I$ to the total energy $E^m$. Setting

$$E^I(\eta)=-i\frac{\gamma^2}{2}\exp\left(-\frac{2}{3}\frac{\gamma^3}{h\eta}\right)=-\frac{ih}{2}D(\eta), \tag{19}$$

$$E^m(\eta)=E_0+E^{\mathrm{ac}}(\eta)+E^I(\eta), \tag{20}$$

the adiabatic development of the ground state can be described by the propagator

$$\hat{U}^{\delta}(t_f)=\exp\left(-\frac{i}{h}\int_0^{t_f}E^m(|\cos(t)|)dt\right)\hat{P}_0, \tag{21}$$

using the total quasienergy $E^m$ and the projection operator $\hat{P}_0$, projecting onto the ground state. This adiabatic description is useful if we want to describe the propagation of the wave function for arbitrary times. If we restrict ourselves to considering only full cycles, we can use the appropriate averages.

$$\overline{E^I}=\left(\frac{3h}{\pi\gamma^3}\right)^{1/2}E^I(\eta=1), \tag{22}$$

$$\overline{E^m}=E_0+\overline{E^{\mathrm{ac}}}+\overline{E^I}, \tag{23}$$

$$\widehat{\overline{U^{\delta}}}(t_f)=\exp\left(-\frac{i}{h}\overline{E^m}t_f\right)\hat{P}_0. \tag{24}$$

By applying this propagator to the ground state and by taking absolute squares, we obtain just the exponential decay with rate $\overline{D}$. This will be sufficient for the forthcoming considerations. For $t_f=2k\pi, k=0,1,2,\ldots$, both propagators are of course identical, due to the very construction of the average.

When comparing these expressions with the numerical results described later, we will see that they can account for the monotonic background of the ionization rate (see Fig. 1). But if we want to explain the superposed modulations, which are responsible for the nonmonotonicity of the rate, we have to go further in our semiclassical description.

## V. SEMICLASSICAL PROPAGATORS

### A. General construction

In order to construct the semiclassical propagator outside the binding potential, we start with the (formal) path-integral expression

$$U(x,t_f;y,t_i)=\int_{t_i}^{t_f}\mathcal{D}x(t)\exp\left\{\frac{i}{h}S[x(t)]\right\}, \tag{25}$$

$$S[x(t)]=\int_{t_i}^{t_f}L(x(t),\dot{x}(t))dt, \tag{26}$$

$$L=T-V=L_0-V_\delta=T-V_0-V_\delta. \tag{27}$$

Here $T$ is the kinetic-energy operator, $L$ is the full Lagrangian, and $L_0$ is the Lagrangian for the electric field $V_0$ alone, without the binding potential $V_\delta$. The usual procedure in the semiclassical limit $h\to 0$ consists in finding the stationary paths with $\delta S=0$. This yields the classical paths by means of the Euler-Lagrange equation [33]. The remarkable point here is that $V_\delta=-h\gamma\delta$ contains a factor $h$. This becomes important in the semiclassical limit, because this $h$ cancels in the exponent $iS/h$. Consequently this part of the phase does no more fluctuate arbitrarily fast for nonstationary paths in the semiclassical limit.

Applying (the analogy to) saddle-point integration in function space, we notice that we only have to vary $S_0=\int L_0$ in order to find the stationary paths to $\delta S_0=0$. This condition gives the classical path $x_{cl}(t)$ to $L_0$ by means of the Euler-Lagrange equation

$$\frac{d}{dt}\left(\frac{\partial}{\partial\dot{x}}L_0\right)-\frac{\partial}{\partial x}L_0=0, \tag{28}$$

subject to the boundary conditions imposed by the path integral.

$$x_{cl}(t_i)=y,\quad x_{cl}(t_f)=x, \tag{29}$$

$$x_{cl}(t)=x_{cl}(t|x,t_f;y,t_i), \tag{30}$$

$$=-\cos(t)+\cos(t_i)+y+\frac{x-y+\cos(t_f)-\cos(t_i)}{t_f-t_i}(t-t_i). \tag{31}$$

Then $V_\delta$ in the full Lagrangian $L$ only accounts for an additional phase factor $\exp(i\gamma\phi)$ to the propagator

$$\phi=\int_{t_i}^{t_f}\delta(x_{cl}(t))dt, \tag{32}$$

$$= \sum_{t_0^j} 1/|\dot{x}_{cl}(t_0^j)|, \tag{33}$$

where the $t_0^j$ denote the zeros of the classical path $x_{cl}(t_0^j)=0$. This phase $\phi$ jumps every time the classical path $x_{cl}(t|x,t_f;y,t_i)$ crosses the $\delta$ potential at the origin.

The result for the semiclassical propagator $U^{sc}$ is

$$U^{sc}(x,t_f;y,t_i) = \frac{1}{\sqrt{2\pi i h}}\left(-\frac{\partial^2}{\partial x \partial y} S_0\right)^{1/2} \times \exp\left(\frac{i}{h} S_0\right) \exp(i\gamma\phi), \tag{34}$$

$$= \frac{1}{\sqrt{2\pi i h (t_f - t_i)}} \times \exp\left[\frac{i}{h}\int_{t_i}^{t_f} L_0(x_{cl}(t),\dot{x}_{cl}(t))dt\right] \times \exp(i\gamma\phi). \tag{35}$$

The same result is derived in Appendix B using the time-dependent WKB ansatz.

In general, one would have to include so-called Maslov phase factors [34], but we can omit them here because we do not encounter any caustics in this problem. Since $V_0 = -x\cos(t)$ is linear in $x$, the appropriate semiclassical propagator for $L_0$ is identical [35] to the exact one, namely, the well-known Volkov propagator $U^V$ [12]. The result can now be understood as the Volkov propagator $U^V$ plus additional phase jumps for every crossing of the origin,

$$U^{sc} = U^V \exp(i\gamma\phi). \tag{36}$$

### B. Special tunneling propagator

There is one important point to note. The construction of the propagator using regular classical paths is only justified after the electron has tunneled out. So in order to include the tunneling paths, which classically do not exist, one has to modify the above description. A common method is to introduce complex time and coordinates (for the mathematical background see [36], for (recent) applications see, e.g., [37,38]). This allows trajectories $x_T$ to pass through regions which are classically forbidden by energy conservation. How this occurs is demonstrated in Appendix C by a simple example.

In our case, we know the bound state $\psi_0 = \sqrt{\gamma/h}\exp(-\gamma|x|/h)$, which formally resembles a plane wave $\exp(ipx/h)$ with complex momentum $p_0 = \pm i\gamma$. This is consistent with a negative energy $E = p_0^2/2 = -\gamma^2/2$, which is just the ground-state energy $E_0$ of the $\delta$ potential.

For the construction of the tunneling propagator $U^T(x,t_f;y,t_0)$, we assume that at time $t_0$ the electron is located at position $y$, with complex momentum $p_0$. We choose the following complex boundary conditions (a similar reasoning appeared in [39]) for the complex tunneling path $x_T$: the initial momentum (imaginary part Im considered only)

$$\mathrm{Im}[\dot{x}_T(t_0)] = p_0 = +i\gamma \tag{37}$$

(the positive sign chosen to ensure exponential decay of wave functions and not growth), and the initial position

$$x_T(t_0) = y. \tag{38}$$

Additionally, $x_T$ must fulfill the final condition

$$x_T(t_f) = x, \tag{39}$$

which is the boundary condition at the end of the path. The additional free constant $t_0$ is necessary because we impose three boundary conditions. But the ordinary differential equation (28), which $x_T$ must obey, is of order 2, and therefore has only two free constants.

The idea is that tunneling takes place in the imaginary part between $t=t_0$ and $t=t_f$. On the other hand, free propagation $U^{sc}$ (under the influence of the oscillating electric field) takes place in the real part. This interpretation is allowed by the usual decomposition rules for semiclassical operators (cf. [40,41]).

The general expression for such a path $x_T$ fulfilling the (now complex valued) equation of motion (28) is

$$x_T(t) = -\cos(t) + \cos(t_0) + y + v_0(t - t_0), \tag{40}$$

$$\dot{x}_T(t) = \sin(t) + v_0. \tag{41}$$

The first condition $\mathrm{Im}[\dot{x}_T(t_0)] = p_0$ yields

$$i\gamma = \mathrm{Im}[\sin(t_0) + v_0]. \tag{42}$$

Now we see the meaning of $t_0$; it must account for the complex boundary condition and so we set

$$t_0 = i\,\mathrm{arcsinh}(\gamma), \tag{43}$$

in order to allow $v_0$ to remain real (see also [39] for this result). The second boundary condition (38) is fulfilled trivially by the ansatz (40), and from the third conditon we obtain

$$v_0 = \frac{x - y + \cos(t_f) - \cos(t_0)}{t_f - t_0}. \tag{44}$$

Using Eqs. (40), (43), and (44), we can easily construct the complete propagator $U^T$ which describes tunneling as well as normal propagation in the electric field. The result is just the analytic continuation of our former result $U^{sc}$ in Eq. (35)

$$U^T(x,t_f;y,t_0) = \frac{1}{\sqrt{2\pi i h (t_f - t_0)}} \times \exp\left[\frac{i}{h}\int_{t_0}^{t_f} L_0(x_T(t),\dot{x}_T(t))dt\right] \times \exp(i\gamma\phi[x_T]). \tag{45}$$

Note that the argument of the square root in the denominator is now truly complex, so that we have an ambiguity in choosing a certain sheet of the complex root. We decide to define $\sqrt{r\exp(i\varphi)} = -\sqrt{r}\exp(i\varphi/2), \varphi \in [0,2\pi]$. Note further

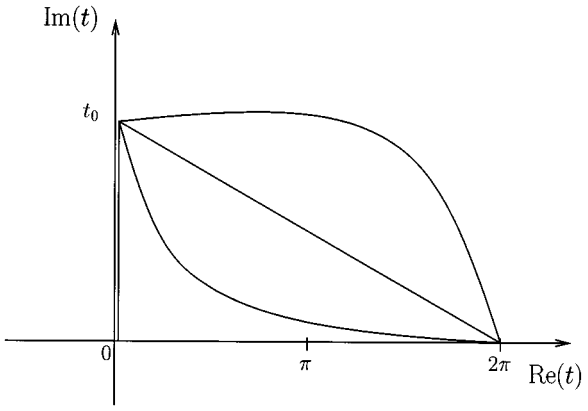


FIG. 2. Path in the complex $t$ plane, describing the evolution of the first wave packet stemming from $t=0$. Since the line integral for the calculation of the semiclassical propagator is path independent, these paths can be chosen at random. It is important that the propagation from $t=0$ to $t=t_0$ uses another propagator (namely, $\widehat{\overline{U^{\delta}}}$) than the propagation from $t_0$ to $t_f=2\pi$ afterwards (with propagator $\hat{U}^T$).

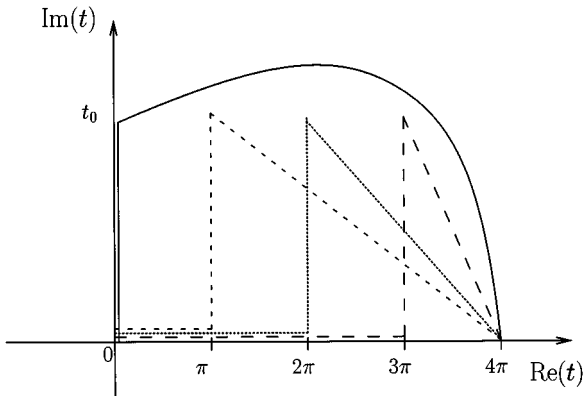


FIG. 3. The various paths in the complex $t$ plane are depicted for four wave packets. The path for the wave packet emerging at $k\pi$ goes from 0 to $k\pi+t_0$ and afterwards to $t_f=4\pi$. Again we have path independence for the two parts.

that the propagator $U^T$ starts at $t_0=i\,\mathrm{arcsinh}(\gamma)$. In order to reach $t_0$, we first have to propagate the ground state from $t=0$ to $t_0$, using $\widehat{\overline{U^{\delta}}}(t_0)$ which is the analytic continuation in time of Eq. (24). This path in the complex $t$ plane is depicted in Fig. 2.

According to the composition rule for propagators, the complete propagator $\hat{U}^c$ for the ground state from $t=0$ to $t_f$ is

$$\hat{U}^c(t_f,0)=\hat{U}^T(t_f,t_0)\widehat{\overline{U^{\delta}}}(t_0) \tag{46}$$

or in coordinate representation

$$\hat{U}^c(x,t_f;y,0)=\int_{-\infty}^{+\infty}\hat{U}^T(x,t_f;z,t_0)\widehat{\overline{U^{\delta}}}(z,t_0;y,0)dz. \tag{47}$$

### C. Generalization to other ionization bursts

The result of the preceding section can be easily generalized to later ionization bursts. Figure 2 shows in the complex $t$ plane that the electron does not become instantaneously free. It propagates from $t=0$ to $t=t_0$ under the propagator $\widehat{\overline{U^{\delta}}}(t_0)$ (valid inside the binding potential), and then it tunnels and propagates from $t_0$ to $t_f=2\pi$ according to the complex-valued propagator $\hat{U}^T$. The line integrals along the depicted paths are path independent [36], so there does not exist a unique path. The important point is that the time evolution consists of different propagators with distinct starting points and with distinct end points. This describes the first ionization burst, but in order to describe the wave packets emerging from the bursts at times $t_k=k\pi$ ($k=0,1,2,3,\ldots,k\pi<t_f$), one can repeat the above calculations.

The propagator $\hat{U}_k^c(t_f,0)$ for the wave packet stemming from $t=k\pi$ is just

$$\hat{U}_k^c(t_f,0)=\hat{U}^T(t_f,k\pi+t_0)\widehat{\overline{U^{\delta}}}(k\pi+t_0). \tag{48}$$

In this notation, $\hat{U}_0^c$ is identical to the above $\hat{U}^c$. The interpretation is that the electron remains bound from $t=0$ to $t=k\pi$. It then propagates into the complex $t$ plane up to $t=k\pi+t_0$, according to $\widehat{\overline{U^{\delta}}}$. After this, it tunnels and propagates from $t=k\pi+t_0$ to $t=t_f$, according to $\hat{U}^T$ (45) (i.e., the complexified Volkov propagator plus phase jumps). Figure 3 contains the four paths corresponding to four wave packets created at $t=0,\pi,2\pi,3\pi$, which interfere at $t_f=4\pi$.

## VI. INTERFERENCE BETWEEN PATHS

The electron has two possibilities, it can tunnel and propagate, or it can remain bound by the binding potential. The quantum-mechanical amplitudes for both processes are known and they can be added in order to obtain a better description of the time evolution of the system. This is just the ''semiclassical sum over classical paths'' method.

The full propagator $\hat{U}$ is the sum of the propagator $\widehat{\overline{U^{\delta}}}$, valid for the electron bound by the $\delta$ potential, and the $\hat{U}_k^c$'s, the propagators for tunneling at $t=k\pi$ and (free) propagation afterwards.

$$\hat{U}(t_f,0)=\widehat{\overline{U^{\delta}}}(t_f)+\sum_{k=0,1,2,\ldots}\hat{U}_k^c(t_f,0). \tag{49}$$

### A. First period

For simplicity and notational reasons, we will at first consider only the wave packet originating from the ionization burst at $t=0$. The other wave packets can be considered in a similar way, and the resulting integrals can be evaluated using the same techniques as described below. We will restrict ourselves to examining the wave function after full periods $t_f=2n\pi$, and we will deal mostly with one single period. The second burst occuring at $t=\pi$ during the first period is of secondary importance, because this free electron follows a classical trajectory $x_{cl}=a+b(t-\pi)-1-\cos(t)$, and its cen-

ter is about $-2$ to the left at $t_f=2n\pi$. Therefore the overlap of this wave packet with the ground state $\psi_0$ can be neglected.

This effect, as well as the influence of considering several periods and wave packets, will be demonstrated when we compare the analytic expressions derived below with numerical results in Sec. VII A.

The propagator (49) must be applied to the ground state $\psi_0$ (5) in order to obtain the wave function $\psi(t_f)$ at a certain time $t_f$

$$\psi(t_f)=\hat{U}(t_f,0)\psi_0. \tag{50}$$

Applying the propagator $\widehat{\overline{U^{\delta}}}(t)$ results in a phase factor $\exp(-(i\overline{E^m}/h)t)$, and expression (50) simplifies to (for one period $t_f=2\pi$)

$$\psi(x,t_f)=\exp\left(-\frac{i\overline{E^m}}{h}t_f\right)\psi_0(x)+\exp(i\gamma\phi)\times\exp\left(-\frac{i\overline{E^m}}{h}t_0\right)\int_{-\infty}^{+\infty}U^V(x,t_f;y,t_0)\psi_0(y)dy. \tag{51}$$

Using the property (7) that $\psi_0(y)$ approaches the spatial $\delta$ function in the semiclassical limit $h\to 0$, the integral can be evaluated to

$$\psi(x,t_f)=\exp\left(-\frac{i\overline{E^m}}{h}t_f\right)\psi_0(x)+\exp(i\gamma\phi)\times\exp\left(-\frac{i\overline{E^m}}{h}t_0\right)2\left(\frac{h}{\gamma}\right)^{1/2}U^V(x,t_f;0,t_0). \tag{52}$$

In order to calculate the probability amplitude $p$ for the electron remaining bound, one has to project onto the ground state $\psi_0(x)$

$$p=\int_{-\infty}^{+\infty}\psi(x,t_f)\psi_0^*(x)dx. \tag{53}$$

Using the normalization of $\psi_0$ and the spatial localization property (7) again, this simplifies to

$$p=\exp\left(-\frac{i\overline{E^m}}{h}t_f\right)+\exp\left(-\frac{i\overline{E^m}}{h}t_0\right)4\frac{h}{\gamma}U^V(0,t_f;0,t_0). \tag{54}$$

$\overline{E^m}$ and $t_0$ are known from Eqs. (23) and (43), respectively. The phase $\phi$ is identical to 0 because the relevant classical path $x_{cl}=1-\cos(t)$ never crosses the origin. The first part of this expression clearly accounts for the background, whereas the second part determines the properties of the superposed (slow) modulation.

### B. Fundamental channel closing thresholds

The phase of the first term in Eq. (54) is mainly given by the expression $-E_0t_f/h$, and the phase of the second term is dominated by the action $S^{cl}/h$ along the classical path $x_{cl}=1-\cos(t)$.

$$S^{cl}=\int_0^{t_f}[\dot{x}_{cl}^2(t)+x_{cl}(t)\cos(t)]dt=-zt_f. \tag{55}$$

The last identity is straightforward (also in atomic units). Combining the phases and comparing them to multiples of $2\pi$ results (for $t_f=2\pi$) exactly in Eq. (8) with $E_{kin}=0$. This is just the threshold condition for channel closing, and this therefore implies the same dependence on $z$. The difference in $z$ between two channel closing thresholds is $\Delta z=1/(1+2\gamma^2)$, if $\gamma$ is kept fixed. Otherwise, if the depth of the binding potential $\alpha$ is kept fixed, the difference in $z$ is $\Delta z=1$ (see Fig. 7 later).

### C. More periods

Again this result can be generalized easily to more bursts and longer final times $t_f>2\pi$. Be $t_f=2n\pi$, then one has to sum over $2n$ bursts and amplitudes, and the result for $p$ is (this time written explicitly)

$$p=\exp\left(-\frac{i}{h}\overline{E^m}t_f\right)+\sum_{k=0}^{2n-1}\frac{-4h}{g\sqrt{2i\pi h(t_f-t_0-k\pi)}}\exp(\zeta^k), \tag{56}$$

$$\zeta^k=\frac{-i}{4h(t_f-t_0-k\pi)}[(t_0+k\pi)^2+(t_f-t_0-k\pi)\times\cos(t_0)\sin(t_0)-2(t_0+k\pi)t_f+4\cos(t_0)(-1)^k-2+t_f^2-2\cos^2(t_0)]-\frac{i}{h}\overline{E^m}(t_0+k\pi). \tag{57}$$

Note the useful relations $\cos(t_0)=\sqrt{1+\gamma^2}$ and $\sin(t_0)=i\gamma$. Propagating the system for longer times $t_f>2\pi$ means to have more phase built up in the exponents of Eq. (56). This results in a finer resolution in the ionization rate $\Gamma$; higher frequencies than the basic modulation can be accounted for. How this can explain the fine structure is demonstrated later on in Fig. 6.

In the above sum (56), only the contributions with $k$ even are important. This is because the centers of wave packets stemming from $k$ odd are located at about $-2$ to the left at $t_f=2n\pi$, and therefore the overlap is very small.

### D. Ionization rate

The probability $w$ for not being ionized is now calculated by taking the absolute square $w=|p|^2$. The corresponding ionization rate $\Gamma$, fitting the exponential decay $w=\exp(-\Gamma t_f/(2\pi))$, can be defined as

$$\Gamma=-\frac{2\pi}{t_f}\ln(|p|^2). \tag{58}$$

In the following, we compare the above semiclassical results for $\Gamma$ with the results from numerical simulations [1].

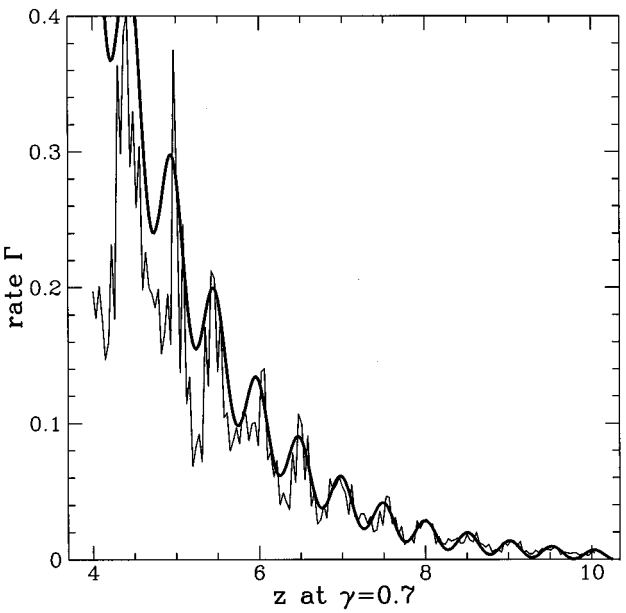


FIG. 4. Numerical ionization rate (thin and jagged) and semiclassical approximation (thick and smooth) vs number of ponderomotive photons $z$ for $\gamma=0.7$.

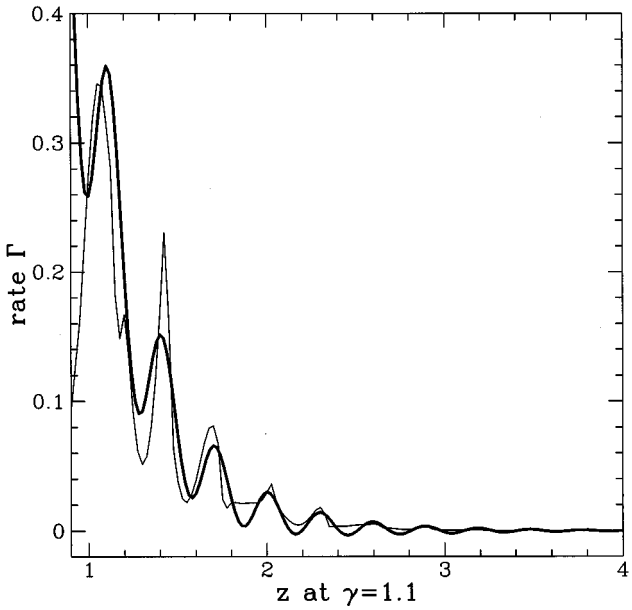


FIG. 5. Numerical ionization rate (thin and jagged) and semiclassical approximation (thick and smooth) vs number of ponderomotive photons $z$ for $\gamma=1.1$.

## VII. COMPARISONS

### A. Comparison with numerical results

The numerical results are obtained by an integral equation method, implemented by Sonnenmoser ( [1] for details). This allows high-resolution scans and exhibits a lot of fine structure. While $\gamma$ is kept fixed, $z$ is varied, and so the semiclassical limit $h\to 0$ corresponds just to $z\to\infty$. This means that the agreement will become better the larger $z$ is.

The interesting region for $\gamma$ is, of course, $\gamma\approx 1$, because this is the transition region between adiabaticity and multiphoton regime. For $\gamma\ll 1$, the adiabaticity criterion is fulfilled. In this case, the averaged WKB value $D$ can be justified, and is in good agreement due to the very construction of our theory. For $\gamma\gg 1$, one should better choose a pure multiphoton description [25,26].

Figure 4 shows the numerical result (thin and jagged) for $\gamma=0.7$, together with the results of our theory. The background as well as the properties of the modulation are very well comprised in the semiclassical theory for $z$ not too small.

The same is done in Fig. 5 for $\gamma=1.1$. Here again, one recognizes that the characteristic elements of the ionization curves are in good agreement. The same is valid for all other values $\gamma\approx 1$ and this result can be extended up to $\gamma\approx 2.5$, clearly beyond the adiabaticity regime.

If we want to incorporate more fine structure superposed onto the modulation, we can consider longer periods than $2\pi$. The result is a behavior like that in Fig. 6. This resembles closely the fine structure, though there can be no one-to-one correspondence with every small wiggle. Here the wave packets stemming from ionization bursts $\pi$ and $3\pi$ were also taken into account, but they have very little influence on the result for $t_f=4\pi$. The main contributions come, of course, from the wave packets stemming from $t=0$ and $t=2\pi$. This can be considered as an example for the qualitative statement above, describing the relative importance of ionization at times that are even or odd multiples of $\pi$.

The result (56) for fixed $\gamma$ and $z$ can easily be transcribed to other parameter combinations. A common representation of ionization rates $\Gamma$ is to keep $n_{io}=2\gamma^2 z=\alpha^2/(2\omega)$ fixed, i.e., the depth of the binding potential (the last expression in atomic units, as in Sec. II A). One varies the intensity $\mu^2$ at fixed frequency $\omega$, which corresponds better to experimental situations. If one plots $\Gamma$ versus the intensity or versus $z=\mu^2/(4\omega^2)$, one again obtains equidistant thresholds with

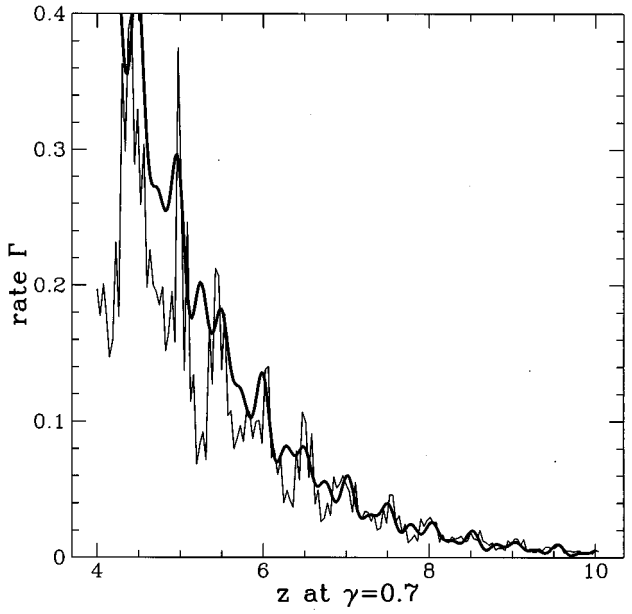


FIG. 6. More fine structure by considering more periods of the external field. Here two cycles ($t_f=4\pi$) are considered.

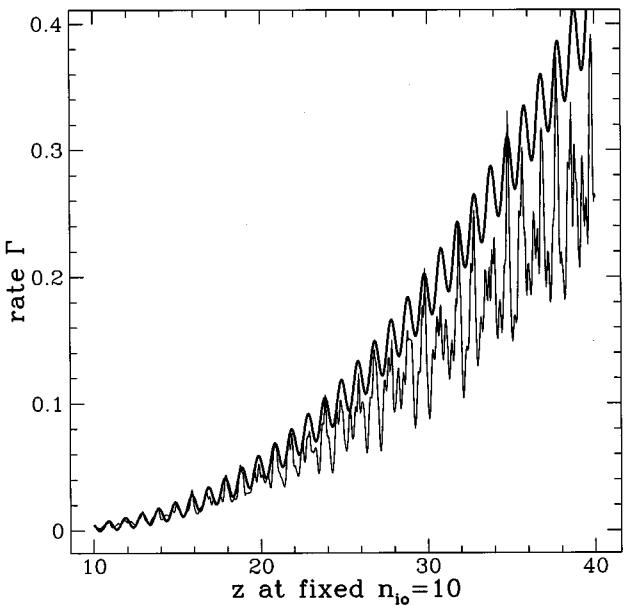


FIG. 7. Now the depth of the binding potential is kept fixed, and z is varied. The semiclassical theory (thick smooth curve) is compared to numerical results (thin and jagged).

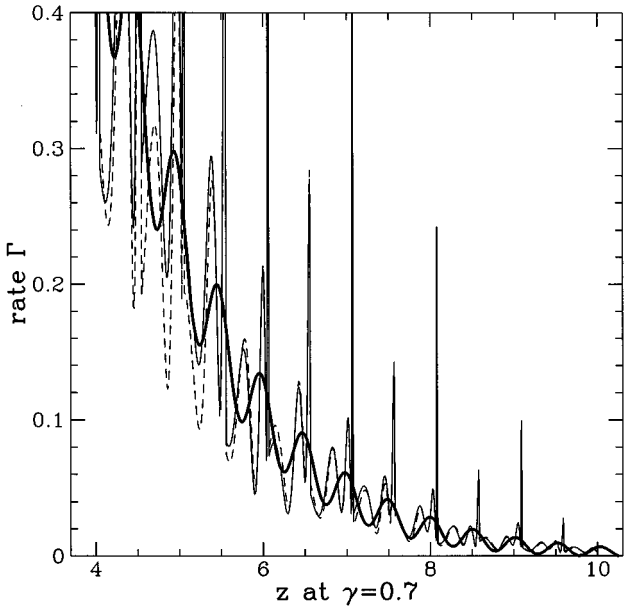


FIG. 8. Comparison with other theories containing divergencies at channel closing thresholds: semiclassical theory (thick and smooth) vs Perelomov, Popov, and Terent'ev [13] (thin line) and Susskind, Cowley, and Valeo [14] (dashed). These two theories nearly coincide between the channel closing thresholds.

$\Delta z = 1$ by ponderomotive channel closing [27]. This is depicted in Fig. 7, together with numerical data. Note that the semiclassical limit no more corresponds simply to $z \to \infty$, but is more involved and cannot be included simply into the representation. One again notices that the characteristic elements of ionization curves can be calculated in the semiclassical theory.

### B. Comparison with other theories

One major advantage and distinction of our theory from others (even from those claiming to be semi- or quasiclassic in some sense) is that we encounter no divergencies of ionization rates at channel closing thresholds, a result strongly supported by numerical evidence. Such divergencies typically occur in theories that (somehow artificially) separate the ionization process into different channels, each one related to ionization by a distinct number of photons. Every time a channel closes, the corresponding ionization rate of the next higher channel (and so the overall rate) becomes infinite.

One earlier representative (Eq. (31) by Perelomov, Popov, and Terent'ev [13]; including quasiclassical features) and one more recent representative [Eq. (44)] by Susskind, Cowley, and Valeo [14]; asymptotic in the number of photons required for ionization) of this kind of theory is shown in Fig. 8, in comparison with our result. The spikes in this figure are related to the closing of certain ionization channels with, say, $k$ photons at $z = z_k$ [Eq. (10)], and they can be traced back to the divergence in the next higher channel with $k+1$ photons.

In between these channel closing events, the background and the imposed modulation is approximately the same for all three theories. But in contrast to these more implicit theories, where results are quite involved, our result [Eqs. (56) and (58)] allows the direct, separate, and explicit evaluation of the background rate as well as of the amplitude and phase of the modulation.

## VIII. SUMMARY

We succeeded in a semiclassical description of time-dependent tunneling and ionization in an oscillating field. The characteristic features of typical ionization curves can now be explained using a picture of tunneling, propagating and interfering wave packets [Eq. (56)]. The main ingredients are, first, the separation of the ionization process into two distinct steps, motivated by the asymptotic evaluation of instantaneous WKB rates. And, second, the usage of complex time and analytical continuation of propagators, necessary to account for tunneling by a classical path description. The slow modulation with channel closing thresholds (an idea stemming from a multiphoton viewpoint) can be described correctly with respect to amplitude and phase. Even the rich superposed fine structure can be accounted for by considering a multitude of interfering wave packets.

## ACKNOWLEDGMENTS

G. Scharf is thanked for valuable discussions and suggestions at all stages of this work. The numerical calculations used for comparison were done with a program packet kindly supplied by K. Sonnenmoser, who is also thanked for two valuable discussions. This work was supported by Schweizerischer Nationalfonds.

## APPENDIX A: EXTENSIBILITY AND COMPARISON TO OTHER MODELS

In Sec. II B, there was explicit use made of the scaling property $\delta(\beta x) = \delta(x)/\beta$ (for $\beta > 0$) of the one-dimensional

$\delta$ function. For the Coulomb potential $V_C$, the scaling behavior is identical, so that the whole calculation can be repeated. The main difference consists in a different phase factor $\phi_C$ [cf. Eq. (32)], which is now the line integral over the Coulomb potential:

$$\phi_C = \int_{t_i}^{t_f} V_C(x_{cl}(t))dt. \tag{A1}$$

This is due to the fact that the binding potential is suppressed by a factor $h$ in the transformed Schrödinger equation (4). As derived in Secs. V A and Appendix B, such a suitably suppressed binding potential does not influence the classical trajectories, but only changes the phase transported along these trajectories by an additional phase factor $\phi_C$ (given above).

This separation is no longer valid for other types of potentials with different (or without) scaling properties. Here the classical equations of motion must be solved fully for the binding potential plus the electromagnetic field. In the time-dependent case, there generally does not exist a first integral of motion (like the energy in the static case), and so the classical system is not integrable in closed form.

The physics of the ionization process should remain the same: complex time-dependent tunneling followed by free propagation (two-step models). This is reflected by the fact that ionization curves for other model potentials show qualitatively the same characteristics (and even quantitatively, see the remark in Sec. III). The semiclassical ''sum over classical paths'' method claims to work in this case anyway, but unfortunately this cannot be done in analytical closed form because of the nonintegrability already on the classical level.

## APPENDIX B: SEMICLASSICAL PROPAGATOR USING THE WKB ANSATZ

This is an alternative to the construction of the semiclassical propagator $U^{sc}(x,t;y,t_i)$ using the path-intgral approach (cf. Sec. V A). We construct $U^{sc}(x,t;y,t_i)$ in such a way that it fulfills the time-dependent Schrödinger equation (4) with respect to $t$ and $x$ up to $O(h^2)$.

$$ih\frac{\partial}{\partial t}U^{sc} = \hat{H}U^{sc} = \left[-\frac{1}{2}h^2\frac{\partial^2}{\partial x^2} - h\gamma\delta(x) - x\cos(t)\right]U^{sc}, \tag{B1}$$

$$\lim_{t\to t_i} U^{sc}(x,t;y,t_i) = \delta(x-y). \tag{B2}$$

We make the ansatz

$$U = \varphi(x,t;y,t_i)\exp\left[\frac{i}{h}S(x,t;y,t_i)\right] \tag{B3}$$

and yield

$$ih\partial_t\varphi - \varphi\partial_t S = \frac{1}{2}(\partial_x S)^2 - ih\partial_x\varphi\partial_x S - \frac{ih}{2}\varphi\partial_x^2 S - \frac{h^2}{2}\partial_x^2\varphi - h\gamma\delta(x)\varphi - x\cos(t)\varphi. \tag{B4}$$

Comparing the distinct orders of $h$:

$$h^0: 0 = \partial_t S + \tfrac{1}{2}(\partial_x S)^2 - x\cos(t), \tag{B5}$$

$$h^1: i\gamma\delta(x)\varphi = \partial_t\varphi + \partial_x\varphi\partial_x S + \tfrac{1}{2}\varphi\partial_x^2 S, \tag{B6}$$

$$2i\gamma\delta(x)\varphi^2 = \frac{\partial}{\partial t}\varphi^2 + \frac{\partial}{\partial x}(\varphi^2\partial_x S). \tag{B7}$$

The right-hand side of Eq. (B7) is just a conservation equation with density $\varphi^2$ and flow $\varphi^2\partial_x S$, which is fulfilled everywhere except the origin. Equation (B5) for $h^0$ is easily solvable, it is just the Hamilton-Jacobi equation $-\partial_t S = H(x,\partial_x S)$ for the motion of an electron in an oscillating electric field (with Lagrangian $L_0$). One can easily solve the appropriate equation of motion and yields the classical path $x_{cl}(\tau)$ with boundary conditions $x_{cl}(t) = x$ and $x_{cl}(t_i) = y$,

$$x_{cl}(\tau) = -\cos(\tau) + \cos(t_i) + y + \frac{x - y + \cos(t) - \cos(t_i)}{t - t_i}(\tau - t_i). \tag{B8}$$

The action $S$ is the time integral over the classical Lagrangian $L_0$

$$S = \int_{t_i}^{t} L_0(x_{cl}(t'), \dot{x}_{cl}(t'))dt'. \tag{B9}$$

Then, as usual, the expression $\varphi_0 = \sqrt{-\partial_x\partial_y S} = 1/\sqrt{t - t_i}$ solves Eq. (B6) for $h^1$ outside the origin. Now we make the ansatz

$$\varphi = \beta(x,t;y,t_i)\varphi_0 = \frac{\beta}{\sqrt{t - t_i}}. \tag{B10}$$

Inserting this in Eq. (B6), we yield

$$i\gamma\delta(x)\beta = \partial_t\beta + \partial_x\beta\partial_x S. \tag{B11}$$

This linear partial differential equation of first order can be solved using the method of characteristics. The (ordinary) differential equation for the characteristic $x_T$ is

$$\frac{d}{dt}x_T = \partial_x S(x,t;y,t_i). \tag{B12}$$

But $S$ is, as we know, the action for the classical path and therefore $\partial_x S$ is just the momentum of the classical path: $\partial_x S = \dot{x}_{cl}(t)$. So we conclude that the characteristic is just the classical path $x_T = x_{cl}$. We obtain the following (ordinary) differential equation for $\beta$ :

$$\frac{d}{dt}\beta|_{x_{cl}} = \partial_t\beta + \partial_x\beta\frac{d}{dt}x_{cl} = i\gamma\delta(x)\beta|_{x_{cl}}. \tag{B13}$$

This can be integrated straightforwardly and the result is

$$\beta(t)|_{x_{cl}} = \exp\left[i\gamma\int_{t_i}^{t}\delta(x_{cl}(t'))dt'\right]\beta_0, \tag{B14}$$

which again can be understood as a phase jump every time the path $x_{cl}(t)$ crosses the $\delta$ potential at the origin. The constant $\beta_0$ can be fixed to $\beta_0=1/\sqrt{2\pi i\hbar}$ by requiring normalization (B2) of $U^{sc}$.

To summarize, we end up with the following result, identical to Eq. (35):

$$U^{sc}(x,t;y,t_i)=\frac{1}{\sqrt{2\pi i\hbar(t-t_i)}}\exp\left(\frac{i}{\hbar}S[x_{cl}](x,t;y,t_i)\right)\times\exp\left(i\gamma\int_{t_i}^{t}\delta(x_{cl}(t'))dt'\right). \tag{B15}$$

## APPENDIX C: COMPLEX TIME DESCRIPTION OF TUNNELING PROCESSES

The usefulness of a complex time coordinate for describing tunneling processes can be demonstrated by a simple example [37]. Consider an inverse harmonic potential barrier $V(x)=-x^2/2$, and a particle coming in from $-\infty$ with energy $E=-1/2$. The classical equation of motion $\ddot{x}_{cl}=x_{cl}$ is fulfilled by the classical trajectory $x_{cl}(t)=-\cosh(t)$, restricting the particle to $x_{cl}\leqslant -1$.

In this time-independent problem, the total energy $E$ is a constant of motion

$$E=\frac{\dot{x}^2}{2}-\frac{1}{2}x^2=-\frac{1}{2}. \tag{C1}$$

This differential equation can be solved for $t(x)$

$$t(x)=\pm\int_{-1}^{x}\frac{dx'}{\sqrt{2E+x'^2}}. \tag{C2}$$

The range of $x$ can now be extended formally to $x>-1$, then $t$ acquires an imaginary part for $x\in[-1,1]$. After the electron has tunneled through the barrier at $x=1$, the imaginary part of the time $t$ is

$$\int_{-1}^{1}\frac{dx'}{\sqrt{2E+x'^2}}=i\pi. \tag{C3}$$

After the tunneling, i.e., for $x>1$, only the real part of $t$ increases, the imaginary part is fixed at $i\pi$.

One can conclude that the total tunneling trajectory through the barrier can be described in the complex $t$ plane by the path $(-\infty,0],[0,i\pi],[i\pi,+\infty+i\pi)$. The second interval represents the actual tunneling process through the barrier, noting that

$$x_{cl}(i\tau)=-\cosh(i\tau)=-\cos(\tau).$$

The third interval describes the propagation on the other side of the barrier, noting that

$$x_{cl}(t+i\pi)=-\cosh(t+i\pi)=+\cosh(t).$$


[1] G. Scharf, K. Sonnenmoser, and W. F. Wreszinski, Phys. Rev. A **44**, 3250 (1991).
[2] G. Mainfray and C. Manus, Rep. Prog. Phys. **54**, 1333 (1991).
[3] K. Burnett, V. C. Reed, and P. L. Knight, J. Phys. B **26**, 561 (1993).
[4] J. H. Eberly, J. Javanainen, and K. Rzazewski, Phys. Rep. **204**, 331 (1991).
[5] *Atoms in Intense Laser Fields*, edited by M. Gavrila (Academic, Orlando, 1992).
[6] J. Opt. Soc. Am. B **7** (4) (1990), special issue on theory of high-order processes in atoms in intense laser fields, edited by K. Kulander and Anne L'Huillier.
[7] K. Sonnenmoser, J. Phys. B **26**, 457 (1993).
[8] See Fig. 11 in Ref. [1], where experimental results for $H^-$ are compared to theoretical results for the one-dimensional $\delta$-function atom.
[9] L. Keldysh, Zh. Éksp. Teor. Fiz. **47**, 1945 (1964) [Sov. Phys. JETP **20**, 1307 (1965)].
[10] F. Faisal, J. Phys. B **6**, L89 (1973).
[11] H. Reiss, Phys. Rev. A **22**, 1786 (1980).
[12] D. Volkov, Z. Phys. **94**, 250 (1935).
[13] A. M. Perelomov, V. S. Popov, and M. V. Terent'ev, Zh. Eksp. Teor. Fiz. **50**, 1393 (1966) [Sov. Phys. JETP **23**, 924 (1966)].
[14] S. M. Susskind, S. C. Cowley, and E. J. Valeo, Phys. Rev. A **42**, 3090 (1990).
[15] W. Becker, R. R. Schlicher, and M. O. Scully, J. Phys. B **19**, L785 (1986).
[16] K. C. Kulander, K. J. Schafer, and J. L. Krause, in *Proceedings of the Workshop on Super Intense Laser Atom Physics SILAP III, NATO Advanced Study Institute Series B: Physics*, edited by B. Piraux *et al.* (Plenum, New York, 1993).
[17] P. Corkum, Phys. Rev. Lett. **71**, 1994 (1993).
[18] M. Lewenstein, Ph. Balcou, M. Y. Ivanov, A. L'Huillier, and P. B. Corkum, Phys. Rev. A **49**, 2117 (1994).
[19] J. Shirley, Phys. Rev. B **138**, 979 (1965).
[20] S. Chu, Adv. At. Mol. Phys. **21**, 197 (1985).
[21] R. M. Potvliege and R. Shakeshaft, Phys. Rev. A **38**, 4597 (1988).
[22] W. Becker, J. K. McIver, and M. Confer, Phys. Rev. A **40**, 6904 (1989).
[23] I. J. Berson, J. Phys. B **8**, 3078 (1975).
[24] N. L. Manakov and P. L. Rapoport, Zh. Éksp. Teor. Fiz. **69**, 842 (1975) [Sov. Phys. JETP **42**, 430 (1976)].
[25] N. B. Delone and V. P. Krainov, *Multiphoton Processes in Atoms* (Springer, New York, 1994).
[26] F. Faisal, *Theory of Multiphoton Processes* (Plenum Press, New York, 1987).
[27] J. Eberly, J. Phys. B **23**, L619 (1990).
[28] W. G. Greenwood and J. H. Eberly, Phys. Rev. A **43**, 525 (1991).
[29] M. Gutzwiller, *Chaos in Classical and Quantum Mechanics* (Springer, New York, 1990).
[30] W. Elberfeld and M. Kleber, Z. Phys. B **73**, 23 (1988).
[31] M. Pont, R. Shakeshaft, and R. M. Potvliege, Phys. Rev. A **42**, 6969 (1990).
[32] S. Geltman, J. Phys. B. **11**, 3323 (1978).

[33] L. Schulman, *Techniques and Applications of Path Integration* (Wiley, New York, 1981).
[34] V. P. Maslov and M. V. Fedoriuk, *Semi-classical Approximation in Quantum Mechanics* (Reidel, Dordrecht, 1981).
[35] R. P. Feynman and A. R. Hibbs, *Quantum Mechanics and Path Integrals* (McGraw-Hill, New York, 1965).
[36] D. McLaughlin, J. Math. Phys. **13**, 1099 (1972).
[37] M. Child, *Semiclassical Mechanics with Molecular Approximations* (Clarendon, Oxford, 1991).
[38] M. Kira, I. Tittonen, W. K. Laii, and S. Stenholm, Phys. Rev. A **51**, 2826 (1995).
[39] V. S. Popov, V. P. Kuznetov, and A. M. Perelomov, Zh. Éksp. Teor. Fiz. **53**, 331 (1967) [Sov. Phys. JETP **26**, 222 (1968)].
[40] M. V. Berry and K. E. Mount, Rep. Prog. Phys. **35**, 315 (1972).
[41] A. Voros, Ann. Inst. Henri Poincaré **XXIV**, 31 (1976).